Atmos. Meas. Tech. Discuss., 3, 1583–1614, 2010
www.atmos-meas-tech-discuss.net/3/1583/2010/

Atmospheric
Measurement
Techniques
Discussions

Optical properties of a heated aerosol in an urban atmosphere: a case study

J. Backman[1], A. Virkkula[1], T. Petäjä[1], M. Aurela[2], A. Frey[2], and R. Hillamo[2]

[1]Department of Physics, University of Helsinki, P.O. Box 64, 00014, Finland
[2]Finnish Meteorological Institute, P.O. Box 503, 00101, Helsinki, Finland

Received: 19 March 2010 – Accepted: 28 March 2010 – Published: 8 April 2010

Correspondence to: J. Backman (john.backman@helsinki.fi)

Published by Copernicus Publications on behalf of the European Geosciences Union.

Abstract

Light absorption measurements most commonly rely on measurement techniques. These filter-based methods are disturbed by light scattering constituents in the aerosol phase deposited on the filters. Light absorption measurements most commonly rely on filter-based measurement techniques. These methods are disturbed by light scattering constituents in the aerosol phase deposited on the filters. Most light scattering constituents in a sub-micron aerosol are volatile by their nature and they can be volatilized by heating the sample air. This volatilisation significantly alters the optical properties of the urban aerosol and was studied during a short field campaign with two groups of equipment measuring in parallel for six days in April 2009 at the SMEAR III station in Helsinki. When heated, the light scattering constituents were evaporated thus reducing the single-scattering albedo (ϖ_0) of the aerosol by as much as 0.4. With less light scattering constituents in the aerosol phase the mass absorption cross section (MAC) of soot was calculated to be $13.5\pm0.5\,\mathrm{m}^2\,\mathrm{g}^{-1}$ at $\lambda=545\,\mathrm{nm}$. An oven was set to scan different temperatures which revealed the volatility of the urban aerosol at different temperatures as well as the single-scattering albedo's dependence on the non-volatile volume fraction remaining (NVFR). At 50 °C 79±13% of the volume remained while only 46±8% remained at 150 °C and just 23±6% at 280 °C. At 50 °C ϖ_0 was 0.65 ± 0.06, at 150 °C $\varpi_0=0.54\pm0.06$ and at 280 °C $\varpi_0=0.33\pm0.06$. We found that absorption coefficients measured at different temperatures showed a temperature dependency possibly indicating initially different mixing states of the non-volatile constituents.

1 Introduction

Aerosol particles have a direct influence on the climate because they scatter (Cabada et al., 2004) and absorb (Jacobson, 2001) light and they have the ability to indirectly influence the climate when acting as a cloud condensation nuclei (Ramanathan et al., 2001; Rosenfeld et al., 2008). Light absorbing black carbon (BC) aerosols heat the atmosphere and they may be the second most important component of global warming in terms of direct forcing (Jacobson, 2001; Ramanathan and Carmichael, 2008). BC is the most effective and dominant absorber of visible solar radiation in the atmosphere (Petzold and Schönlinner, 2004; Ramanathan and Carmichael, 2008). The internally mixed state of BC with aerosol constituents can enhance forcing by a factor of two (Jacobson, 2001). BC emissions are mainly anthropogenic. The highest emissions are in the tropics where the incoming solar radiation is the strongest (Ramanathan and Carmichael, 2008).

Soot is externally mixed when it is introduced in to the atmosphere, but during transport, the soot particles coagulate with other particles or get coated with sulphates, nitrates or organic species by condensation (Saathoff et al., 2003; Zhang et al., 2008). This results in different mixing states of BC. Absorption of light in aerosols has been studied for a long time but there are still uncertainties which affect the accuracy of climate models (Bond and Bergstrom, 2006).

The most commonly used filter-based measurement techniques for determining absorption of light in an aerosol is disturbed by light scattering aerosols (e.g. Bond et al., 1999; Virkkula et al., 2005). Volatile compounds such as sulphates, nitrates and most of the organic species are evaporated at temperatures around 300 °C (Engler et al., 2007; Tiitta et al., 2009). At these temperatures BC is still non-volatile (Wehner et al., 2005). The residual particles at this temperature consist of soot, crustal material or sea salt (Frey et al., 2008). Exluding these compounds, the light scattering constituents in the aerosol phase are volatile. Thus, the disturbance due to the light scattering material to absorption can be reduced by heating the sample air. In practice this can be done by letting the sample air pass through a thermodenuder (Wehner et al., 2002). The amount of evaporated material from the aerosol phase depends on the composition of the particles and is also a function of the time the sample air spends inside the thermodenuder as well as the temperature of it is heated to (An et al., 2007; Riipinen et al., 2010)

In this study a suite of optical instruments were deployed to the SMEAR III station (Järvi et al., 2009) in Helsinki to measure the optical properties of urban background aerosol with and without a volatilisation oven in front of the instruments for a short field campaign (Backman, 2009). The aim was to show a proof-of-concept that the performance of the filter-based methods can be improved with the aid of volatility analysis, in which the compounds responsible of the scattering are progressively evaporated from the aerosol sample. The absorption after the volatilisation of the oven was measured with a Particle Soot Absorption Photometer (PSAP) along with a nephelometer and size distribution measurements which were compared with non-heated aethalometer, nephelometer, size distribution data as well as with measured elemental and organic carbon content of the ambient particle population.

2 Experimental setup

A suite of instruments were deployed to the SMEAR III station (Järvi et al., 2009) with a purpose to look into aerosol optical properties of the urban aerosol with and without exposing the sampled particles to an elevated temperature. A schematic illustration of the instrument setup is presented in Fig. 1.

The devices with a non-heated sampling line are refered as "non-heated" and "cool" and are measuring at SMEAR III continuously (Järvi et al., 2009). The scattering was determined with a three wavelength nephelometer and absorption with a Magee Scientific Aethalometer. A Twin-Differential Mobility Particle Sizer (Aalto et al., 2001) was monitoring the particle number size distribution. The mass concentration of elemental and organic carbon was determined via thermal-optical analysis with a Sunset ECOC instrument (Birch and Cary, 1996).

The instruments operated with the thermodenuder are hereafter refered to as "heated". This group included a single wavelength nephelometer (Radiance Research Nephelometer M903), a Particle Soot Absorption Photometer (PSAP, Radiance Research) for determining the absorption as well as a Differential Mobility Particle Sizer

(DMPS) for aerosol particle number size distribution measurements. The campaign instruments were taking the sample through a Minnesota PM_{10} inlet approximately three meters from the SMEAR III standard instruments. Prior to the field campaign the operation of the instruments was verified in the laboratory.

The instruments after the thermodenuder (also referred to as oven) were operated at the SMEAR III station for six days between 9–14 April 2009 with a constant 280 °C oven temperature. During the next 24 h period the oven temperature was varied in three steps (50, 150 and 280 °C). A single temperature scan was completed in approximately 2.5 h. A more detailed description of all the instruments is given in the following sections.

2.1 SMEAR III instrumentation (non-heated)

The optical properties with a non-heated inlet was measured using a scatter/backscatter integrating nephelometer TSI Inc. 3653 (St. Paul, MN, USA) which measures at 450, 550 and 700 nm wavelengths (Anderson et al., 1996). The instrument does a geometrical integration of the scattered intensity with a Lambertian light source and an orthogonally orientated detector. The design of the TSI Inc. 3653 allows measurements of backscattering and total scattering by aerosols but only total scattering coefficients were used in this study. The data had a time resolution of one minute.

Light absorption coefficients were calculated from a Magee Scientific Aethalometer AE-16 (Berkeley, CA, USA) measuring at a wavelength of 880 nm (Hansen et al., 1984; Arnott et al., 2005). This instrument uses a filter-based optical method for estimating the BC concentration which can be used to calculate absorption coefficients (Arnott et al., 2005). This instrument had a time resolution of five minutes.

The ambient particle number size distribution between 3 to 950 nm was measured with a Twin-Differential Mobility Particle Sizer (TDMPS, Aalto et al., 2001). The TDMPS consisted of two Hauke-type (Winklmayr et al., 1991) differential mobility analyzers (DMA) with closed loops for the sheet air flows (Jokinen, 1995) connected to a Condensation Particle Counter (CPC). The first DMPS system measured from 3–50 nm with a TSI 3025 CPC, (Stolzenburg and McMurry, 1991) and the second from 10 to 950 nm with a TSI 3010 CPC, (Mertes et al., 1995). The combined number size distribution from 3 to 950 nm was obtained with a ten minute time resolution.

Elemental carbon (EC) and Organic Carbon (OC) mass concentrations were measured with a Sunset Laboratory OCEC M3F (Tigard, OR, USA) via thermal-optical analysis (Birch and Cary, 1996). This is done by deposition of particles on a quartz filter by heating the sample subsequently in two different atmospheres (helium and helium plus oxygen). In the pure He atmosphere the sample is heated in steps to evolve the collected OC via pyrolysis, thus making the filter darker while monitoring the filter transmittance. In the next step the oven is cooled and the EC and pyrolysed OC is exposed to $He-O_2$ mixture. From the detected combustion products the amount of OC and EC can be determined. The amount of EC is determined after the filter transmittance returns to its initial value. The OCEC analyzer had a time resolution of one hour.

2.2 Campaign instrumentation (heated)

An oven was used to evaporate the volatile constituents from the aerosol. It consisted of a stainless steel tube surrounded with a heating cable. The oven temperature was controlled with a computer through a Drew Scientific 5310 proportional-integral-derivative (PID) controller. The time resolution in scanning the temperatures was poor due to large thermal mass of the oven incorporated with insufficient cooling. Thus the oven was operated at a constant 280 °C temperature for the beginning of the campaign and a short test of varying the temperature was conducted at the end of the campaign. In the initial laboratory the residence time of the aerosol in the oven was 1.2 s and during the campaign it was 1.0 s. Although this probably is not long enough to fully evaporate the volatile material from the aerosol phase (Riipinen et al., 2010), it is still much longer than e.g. 0.3 s residence time used in the study by Philippin et al. (2004).

The optical properties of the heated sample was done with an integrating nephelometer (Radiance Research Inc., Seattle, WA, USA) M903 that measured total light scattering coefficients at a wavelength of 545 nm (Liu et al., 2002; Heintzenberg et al., 2005). The absorption coefficients were determined with a three wavelength Particle Soot Absorption Photometer (PSAP, Radiance Research Inc., Seattle, WA, USA) measuring at 467, 530 and 660 nm (Virkkula et al., 2005).

The aerosol number size distribution after heating were measured with a DMPS from 10 to 600 nm particle sizes (Hoppel, 1978; Aalto et al., 2001). The DMPS consisted of a 28 cm Hauke-type DMA (Winklmayr et al., 1991) with closed loop flow arrangements (Jokinen, 1995) and a TSI Inc. 3010 CPC (Mertes et al., 1995) for particle counting. In this systems sample and sheet air flows were set to 0.9 and 7.4 $\mathrm{l\,min^{-1}}$. The time resolution was 10 min.

For comparison between the campaign instruments and the SMEAR III instruments, the oven was switched off at the end of the campaign period. This enabled us to verify the performance of the campaign devices.

2.3 Data processing

Both the PSAP and the Aethalometer use a filter-based method for measuring light absorption by attenuation of light transmitted through a filter matrix while particulate matter is collected onto the filter resulting in a reduction in the light transmission. An uncorrected absorption coefficient is obtained from

$$\sigma_0 = \frac{A}{V} \ln\left(\frac{I_{t-\Delta t}}{I_t}\right), \tag{1}$$

where A is the area of the sample spot, V is the volume of the air that passes the filter in the time Δt. $I_{t-\Delta t}$ and I_t are the light transmission through the filter before and after the time Δt has elapsed. This relationship, however, changes as the filter gets loaded with both light absorbing and light scattering aerosol particles. Procedures for correcting for various effects are presented in Bond et al. (1999); Weingartner et al. (2003); Arnott et al. (2005), and in Virkkula et al. (2005). The light scattering aerosol deposited onto the filter gets wrongly interpreted as absorption, if not taken into account.

Generally, the absorption coefficient σ_{AP} is calculated from

$$\sigma_{AP} = f\sigma_0 - s\sigma_{SP}, \tag{2}$$

where f is a correction factor that depends on both the amount and also on the darkness of the deposited aerosol material. The σ_{SP} is the scattering coefficient and s is the fraction of scattering that is interpreted as absorption. In order to correct for this also σ_{SP} has to be measured, preferably at the same wavelength as σ_0 was measured at. If the two parameters are derived at different wavelengths λ_1 and λ_2, either of them has to be interpolated or extrapolated to the matching wavelength with the aid of the Ångström exponent

$$\alpha_{12} = -\frac{\log(\sigma_1/\sigma_2)}{\log(\lambda_1/\lambda_2)}, \tag{3}$$

which describes the wavelength dependency of the scattering and absorption. The Ångström exponent can be used to relate the data to the same wavelength (λ_x) with

$$\sigma_x = \sigma_1 \left(\frac{\lambda_1}{\lambda_x}\right)^{\alpha_{12}} \tag{4}$$

This requires the assumption that the spectral dependence of the Ångström exponent is constant.

By using Eqs. (3) and (4), the coefficients can be interpolated or extrapolated to a arbitrary wavelength if they were measured at different wavelengths. In this study, the PSAP light absorption coefficient data were interpolated using this method to the same wavelength as the M903 nephelometer measured at. The TSI nephelometer light scattering coefficient data were extrapolated to the same wavelength as the Aethalometer measured at (880 nm).

The ratio of scattered light to light extinction by particles is called single-scattering albedo, defined as

$$\omega_0(\lambda) = \frac{\sigma_{SP}(\lambda)}{\sigma_{SP}(\lambda)+\sigma_{AP}(\lambda)} = \frac{\sigma_{SP}(\lambda)}{\sigma_{ext}(\lambda)}. \tag{5}$$

The ω_0 depends on the aerosol size distribution and on the chemical composition and is also wavelength dependent. It is the key parameter governing the amount of cooling or heating an atmospheric aerosol layer can induce (Seinfeld and Pandis, 2006).

2.3.1 PSAP data

The methods used in this study for compensating for the PSAP transmittance decrease and for scattering aerosols is described in Virkkula et al. (2005) and in Virkkula (2010). It is an iterative method which takes the darkness of the aerosol deposited on the filter into account. Initially ω_0 is calculated from the raw count data produced by the PSAP and σ_{AP} was calculated using an iterative procedure

$$\sigma_{AP} = (k_0 + k_1(h_0 + h_1\omega_0)\ln(\mathrm{Tr}))\sigma_{AP} - s\sigma_{SP} \tag{6}$$

where the factors k_0, k_1, h_0, h_1, and s are the constants presented in Table 1. A limit for convergence was set to 0.01 Mm^{-1}, which was typically achieved after 2–3 cycles. The values of the coefficients used here were calculated for 530 nm but were now used for absorption coefficients calculated at 545 nm. This inconsistency is thought to be negligible or minor and was not investigated.

This method was also compared with the more commonly used method that is described in Bond et al. (1999) and in Ogren (2010),

$$\sigma_{AP,O10} = \frac{\sigma_0}{1.5557\mathrm{Tr}+1.0227} - 0.0164\sigma_{SP} \tag{7}$$

as derived in Virkkula (2010). This is partly the method the PSAPs firmware uses to calculate the absorption coefficients displayed on the front display of the instrument and that is reported through a serial port. The last term of Eq. (7) corrects for the scattering aerosol deposited on the filter.

Since the Radiance Research M903 is a one wavelength nephelometer, the light absorption coefficients were interpolated to 545 nm using the Ångström exponents calculated between 530 and 660 nm using Eqs. (3) and (4). At 545 nm the correction for light scattering aerosols was done using Eqs. (6) and (7).

2.3.2 Aethalometer data

The Aethalometer estimates black carbon mass concentrations by measuring the change in the attenuation of light through a fibre filter. From these data, the light absorption coefficients can be calculated for example using the algorithms presented in Arnott et al. (2005) or in Weingartner et al. (2003). In this study the algorithm as described in Arnott et al. (2005) was used to convert the mass concentration values to absorption coefficients using

$$\sigma_{\mathrm{AP},n} = \frac{\mathrm{SG\,BC}_n - \alpha\sigma_{\mathrm{SP},n}}{M}\sqrt{1 + \frac{\frac{\mathrm{Vdt}}{A}\sum_{i=1}^{n-1}\sigma_{\mathrm{AP},i}}{\tau_{a,\mathrm{fx}}}}. \qquad (8)$$

The values used in Eq. (8) are presented in Table 2. The values M and $\tau_{a,\mathrm{fx}}$ were calculated assuming the same wavelength dependency for the coefficients as presented in Arnott et al. (2005) using the more suitable values of M=3.688 and $\tau_{a,\mathrm{fx}}$=0.2338 for ambient measurements at a wavelength of 521 nm.

Equation (8) requires that the light scattering coefficients σ_{SP} are determined at the same wavelength at which the BC concentrations were measured. The AE-16 aethalometer uses a 880 nm wavelength so the light scattering coefficients were extrapolated to that wavelength using Eqs. (3) and (4). The extrapolation was done from the Ångström exponents calculated between 550 and 700 nm from the TSI nephelometer data. Due to lower time resolution of the aethalometer, this was done by averaging the nephelopmeter data to five minutes.

Since the TSI nephelometer data had a higher time resolution than the aethalometer the nephelometer data were averaged to match the aethalometers time resolution.

3 Results and discussion

3.1 Verification experiments

Evaporation of volatile material from the particle phase in an oven is a function of the time the aerosol resides in the thermodenuder (An et al., 2007; Riipinen et al., 2010). Prior to utilizing the oven in the field we tested it with laboratory-generated ammonium sulphate $(NH_4)_2SO_4$ and sodium chloride NaCl aerosol. These aerosols were produced with two different nebulizers. The salts were dissolved in deionized water. The humid aerosol was then dried with silica gel before it was led in to the oven.

The residence time of the aerosol in the oven was 1.2 s with a flow of $3.0\,\mathrm{l\,min^{-1}}$. With this flow rate the volatilisation of ammonium sulphate was complete while sodium chloride did not evaporate completely (Fig. 2). The temperature, where 50% of the ammonium sulphate aerosol volume was evaporated, was at 145 °C. The 50% value in terms of particle number occurred already at 130 °C. At 200 °C only 10% of the volume and 1% of the particles survived the oven. The sodium chloride aerosol volume decreased to 80% at 300 °C. Otherwise the thermodenuder did not affect remarkably the volume or number concentration of the sodium chloride particles.

Before deploying the campaign instruments to the SMEAR III station, the PSAP and the Nephelometer M903 were tested in the laboratory. The flow of the PSAP instrument was calibrated with the least squares method curve fitting with a slope of 1.002 ± 0.009 and an offset of 0.017 ± 0.010. The apparent absorption (σ_0) determined with the PSAP were corrected accordingly.

The noise of the PSAP was estimated to be less than 0.65 Mm^{-1} with the formula $\delta\sigma_{\mathrm{AP}} = 10^{0.60-1.31\log(\Delta t)}$ as in Springston and Sedlacek (2007) with an averaging time Δt of 4 s. The noise of the PSAP was later measured to be less that 0.48 Mm^{-1} while sampling particle free air.

The Radiance Research Nephelometer M903 was calibrated using carbon dioxide and particle free air. The noise of the nephelometer was then determined to be less than 0.17 Mm^{-1} with flow rates between one and three litres per minute from 30 min of data.

3.2 Volatility of urban aerosol

Optical properties and BC concentration at SMEAR III station in Finland were monitored from 9 April to 15 April 2009. The experiments were conducted in parallel with the thermodenuder at an elevated temperature and without heating (Fig. 1). At the start of the field campaign the oven was kept at a constant temperature of 280 °C from 9 April LT 11:00 to 14 April LT 10:00. During the last 23 h period of the experiments, from 14 April LT 10:00 to 15 April LT 09:00, the oven temperature was scanned from 50 °C to 280 °C. First we discuss the results at the constant oven temperature and subsequently present the findings with the variable oven temperature, which progressively evaporates volatile material from the particulate phase.

3.2.1 Constant oven temperature

The time series of optical and physical parameters measured during the campaign are presented in Fig. 3.

The heated and cool coefficients σ_{SP} and σ_{AP}, as well as the simultaneously measured OC and EC concentrations are plotted in Fig. 3. The cool scattering coefficient ($\sigma_{\mathrm{SP,TSI}}$) followed closely the OC variations, the heated ($\sigma_{\mathrm{SP,M903}}$) not as well. It is very obvious already from this time series that most of the scattering material is volatile at 280 °C. Both absorption measurements track the EC concentrations and each other, as they should. The difference between the heated and cool σ_{AP} ($\sigma_{\mathrm{AP,PSAP}}$ and $\sigma_{\mathrm{AP,AETH}}$) is mainly due to the different wavelengths although there are some periods with high noise of $\sigma_{\mathrm{AP,PSAP}}$, for instance on the afternoons of 10 April, 11 April, 12 April and 13 April whereas $\sigma_{\mathrm{AP,AETH}}$ was much more stable in these periods. The data do not give a clear and unambiguous explanation to these. In principle one explanation could be that the instrument became noisy after the light transmittance through the filter had decreased to a low level. However, the $\sigma_{\mathrm{AP,PSAP}}$ noise decreased to the normal level for long periods even before the following filter change. Humidity generally creates noise in filter-based instruments but after the oven this is for sure not the case.

The time series of the non-volatile volume fraction remaining (NVFR), single-scattering albedo (ω_0) of the heated and cool aerosol ($\omega_{0,\mathrm{heated}}$ and $\omega_{0,\mathrm{cool}}$ at λ=545 nm and 880 nm, respectively) reveal interesting variations (Fig. 3). First of all, approximately 70% of the aerosol volume had volatilized (NVFR≈0.3) and the difference between the two ω_0:s was >0.3, meaning the residual particles were much darker. This is in agreement with our understanding that in sub-micron aerosol volatile constituents scatter more light than the non-volatile matter.

Secondly, in some periods $\omega_{0,\mathrm{heated}}$ decreased close to 0.3, the ω_0 of soot (e.g., Mikhailov et al., 2006) and even lower. The noisy periods of $\sigma_{\mathrm{AP,PSAP}}$ mentioned above occur interestingly simultaneously with clearly elevated and even somewhat noisy NVFR – with the exception of 13 April – and also clearly decreased values of $\omega_{0,\mathrm{cool}}$ suggesting that the noisy $\sigma_{\mathrm{AP,PSAP}}$ periods may have been due to near-by soot sources. With heavy traffic and local emissions we would expect a diurnal cycle of dark residual aerosols at rush hour and less dark aerosol at night time. Since the campaign was conducted mainly over a national holiday there is no clear diurnal cycle even though the above analysis shows that in this period the dark aerosol was mainly observed in the afternoons and evenings.

The third observation from the time series of NVFR and ω_0 is that there are periods where the residual aerosol has a different ω_0 with roughly the same NVFR. For example NVFR≈0.25 and $\omega_{0,\mathrm{heated}}$ ≈0.3 just after midnight on 12 April. Just after midnight on 13 April NVFR≈0.25 while $\omega_{0,\mathrm{heated}}$ ≈0.5. This is most probably an indication of chemically different aerosols entering the oven. Our laboratory tests showed the oven volatilized ammonium sulphate, other typical inorganic sub-micron aerosol constituents are even more volatile (e.g., Engler et al., 2007; Tiitta et al., 2009). We therefore conclude the non-volatile aerosol probably contained organics, in addition to BC.

In OC/EC analysers the sample is heated stepwise, typically to four different temperatures. For instance, the recommended EUSAAR protocol is to heat the sample to 200, 300, 450, and 650 °C, and in the IMPROVE protocol to 120, 250, 450, and 550 °C (Cavalli et al., 2010) yielding concentrations of OC1, OC2, OC3, and OC4. If there were organics in the volatility ranges OC3 and OC4 present in aerosol our setup would not have volatilized them. The data suggest this has been the case in the period indicated above. However, we can not prove this for sure since from the whole campaign we only have the total OC data, not different temperature fractions. Another explanation would be that in this period the 1.0 residence time in the oven was too short to evaporate all organics (Riipinen et al., 2010).

The residual aerosol is darker than the cool aerosol and therefore there is less scattering aerosol to influence the light absorption measurements. This generally results in a more accurate measure of mass absorption cross sections (MAC) (Bond and Bergstrom, 2006). The MAC of EC was determined with linear regression of σ_{AP} from both absorption measurements vs. the EC mass concentrations from the OC/EC-analyzer. From the aethalometer data MAC=$6.2\pm0.4\,\mathrm{m^2\,g^{-1}}$ (Fig. 4a) at λ=880 nm. At λ=545 nm, the MAC calculated from the heated PSAP data was $13.5\pm0.9\,\mathrm{m^2\,g^{-1}}$ (Fig. 4b). When the Bond et al. (1999) and Ogren (2010) corrections were used, the MAC was $9.6\pm0.5\,\mathrm{m^2\,g^{-1}}$. These results are in agreement with earlier published MAC values (9.1–10.8 $\mathrm{m^2\,g^{-1}}$ and 5–25 $\mathrm{m^2\,g^{-1}}$ (λ=550 nm), 9.8 $\mathrm{m^2\,g^{-1}}$ (λ=565 nm) and 5.9–9.3 $\mathrm{m^2\,g^{-1}}$ (λ=880 nm) (e.g., Petzold and Schönlinner, 2004; Snyder and Schauer, 2007; Miyazaki et al., 2008, and references therein).

3.2.2 Temperature dependence of volatilization

From 14 April 10:00 to 15 April 09:00 the oven was set to cycle temperatures 50, 150 and 280° for 23 h and finally the oven was turned off for a few hours. The time series of scattering and aerosol volume concentration show that even the non-heated aerosol did not remain constant during this scanning period, the volume varied about a decade, from about 2 to 20 $\mu m^3 cm^{-3}$ and $\sigma_{SP,TSI}$ from about 10 to 100 Mm^{-1} (Fig. 5).

Heating made a huge impact on the light scattering properties of the aerosol. The warmer the oven was the more it evaporated light scattering constituents from the aerosol phase. A decrease in σ_{SP} was expected but an interesting observation was that the temperature also influenced σ_{AP}. This same issue may be studied by comparing the absorption coefficients of the cool aerosol to the heated one, $\sigma_{AP,AETH}$ and $\sigma_{AP,PSAP}$, respectively. There are clear differences in the slopes (Fig. 6). One possible explanation is that the scattering correction function by Virkkula et al. (2005) does not compensate for the scattering aerosol deposited on the filter matrix perfectly.

Since the amount of residual scattering aerosol is a function of temperature and light scattering is a variable in the correction function to calculate the absorption the variations in scattering do influence the results. The more likely explanation is that the mixing state of the aerosol changes during heating and therefore changes the absorption properties of the aerosols. It has been shown that the mixing state of soot in an aerosol can increase the amount of radiation the aerosol absorbs by a factor of 2.9 (Jacobson, 2001). The fact that the volatilisation of light scattering matter from the aerosol can influence the light absorption coefficient is a possible indication of internally mixed BC. Soot is externally mixed immediately after emission but gets coated with non-absorbing constituents during transport in the atmosphere. The longer BC has aged the more likely it is that it gets internally mixed with light scattering constituents (Saathoff et al., 2003; Frey et al., 2008; Zhang et al., 2008).

At 50 °C there was already some volatilization, 79 ± 13% of the volume remained while only 46 ± 8% remained at 150 °C and just 23 ± 6% at 280 °C (Fig. 7). $\omega_{0,heated}$

behaved analogically, it was 0.65 ± 0.06 at 50 °C, 0.54 ± 0.06 at 150 °C and 0.33 ± 0.06 at 280 °C. At 280 °C the non-volatile particles had the ω_0 of soot ($\approx$0.3) in most of the scans but in some clearly higher, about 0.4, indicating again possible non-volatile organics. The analogical behaviour of NVFR and $\omega_{0,\text{heated}}$ raises a question of the type of relationship they have. There was a clear decreasing trend in $\omega_{0,\text{heated}}$ as a function of NVFR but it was not quite linear: the ω_0 drop was approximately as large when NVFR dropped from 0.4 to 0.3 as when it dropped from 0.8 to 0.4 (Fig. 8). The reason for this may be the effect of scattering layers around the absorbing core.

For those data where $\omega_0 < 0.3$ NVFR was $\approx 0.25 \pm 0.05$. This is slightly higher than the published volume fractions of BC in $PM_{2.5}$ (Viidanoja et al., 2002; Putaud et al., 2004). This is what we would expect since the non-volatile soot particles are found well beneath the cut off size of $PM_{2.5}$ (Philippin et al., 2004; Engler et al., 2007). Most traffic-related less volatile particles have been shown to be between 80 and 150 nm (Wehner et al., 2004).

We can still get another piece of information out of the $\omega_{0,\text{heated}}$ vs. NVFR plot (Fig. 8). Since the method for calculating σ_{AP} was only calibrated for filter transmittances >0.4 (Virkkula, 2010) the respective data were plotted in green in Fig. 8. The fact that there is no obvious difference between values obtained with Tr<0.4 and Tr>0.4 indicates that the used method seems to be suitable for even lower transmittances than indicated in the original paper.

4 Conclusions

We measured the effect of heating on light scattering and absorption by aerosols at an urban background station in Helsinki from 9 to 15 April 2009. First the heating temperature was kept constant at 280 °C for five days and then temperatures 50, 150, and 280 °C were scanned for 23 h. Heating significantly altered the optical properties of a particle population. The scattering constituents got volatilised resulting in a darker aerosol. The single-scattering albedo of the residual aerosol ($\omega_{0,\text{heated}}$), as well as the non-volatile volume fraction remaining (NVFR), decreased almost linearly as a function of the heating temperature.

The darkening of the aerosol reduces the amount of light scattering material deposited on the filter matrix used to measure light absorption in aerosols. In principle this will result in more accurate absorption measurements since scattering has to be taken into account when calculating absorption from any filter-based absorption measurement instrument. However, the result of this study suggests that it is not necessarily as simple as just removing all scattering material and then getting a non-biased σ_{AP}. The absorption in the filter matrix actually seems to carry information on the mixing state. The fact that there seems to be a temperature dependence of the calculated absorption coefficients is probably an indication of different mixing states of the aerosol achieved by partial, complete or no volatilisation in the oven. Different mixing states of BC have been shown to affect light absorption so that internally mixed aerosol should absorb more light than externally mixed (Jacobson, 2001).

The mass absorption cross section of the heated aerosol was calculated to be $13.5 \pm 0.9\,\mathrm{m^2 g^{-1}}$ at λ=545 nm using the PSAP algorithm presented by Virkkula et al. (2005); Virkkula (2010) and $9.6 \pm 0.5\,\mathrm{m^2\,g^{-1}}$ using the Bond et al. (1999) correction with the modification by Ogren (2010) and the OC/EC data. For the non-heated aerosol MAC=$6.2 \pm 0.4\,\mathrm{m^2\,g^{-1}}$ was calculated from aethalometer data at λ=880 nm. These values are consistent with published values but our data leaves a question open: is this difference in MAC calculated from the two instruments due to wavelength only or is it due to different state of mixing. This should be studied by making both heated and non-heated measurements at equal wavelengths and similar instruments.

An interesting observation is that there were periods where $\omega_{0,\mathrm{heated}}$ increased from about that of soot (≈0.3) to ≈0.4 even though the non-volatile volume fraction remained at about 0.25 and the oven was kept at the constant temperature of 280 °C. A probable explanation to this is that in these periods in the particles there was organic carbon that volatilizes only at higher temperatures, since the typical inorganic sub-micron species get volatilized at this temperature. In the standard thermal-optical

OC/EC analysis there are four temperature steps, two of them yield concentrations of OC that volatilize at temperatures >300 °C (Cavalli et al., 2010). The measurement of $\varpi_{0,\mathrm{heated}}$ and NVFR could possibly be used as an indication of the presence of these organics. How quantitative this would be remains to be studied.

As the PSAP filter gets darker the difference in the absorption coefficients calculated with the logarithmic loading correction function (Virkkula et al., 2005; Virkkula, 2010) and the more commonly used Bond et al. (1999) correction becomes significant. The comparison of the non-volatile volume fraction and single-scattering albedo during the heating temperature cycling period suggests that the logarithmic loading correction function works even at transmittances lower than 0.4.

Acknowledgements. We acknowledge the financial support by the Maj and Tor Nessling foundation under grant 2008400 and 2009399 and the technical assistance of Timo Mäkelä.

References

Aalto, P., Hämeri, K., Becker, E., Weber, R., Salm, J., Mäkelä, J., Hoell, C., O'Dowd, C., Karlsson, H., Hansson, H.-C., Väkevä, M., Koponen, I., Buzorius, G., and Kulmala, M.: Physical characterization of aerosol particles during nucleation events., Tellus, 53B, 344–358, 2001. 1586, 1587, 1589

An, W. J., Pathak, R., Lee, B.-H., and Pandis, S.: Aerosol volatility measurement using an improved thermodenuder: Application to secondary organic aerosol, J. Aerosol Sci., 38, 305–314, 2007. 1585, 1593

Anderson, T., Covert, D., Marshall, S., Laucks, M., Charlson, R., Waggoner, A., Ogren, J., Caldow, R., Holm, R., Quant, F., Sem, G., Wiedensohler, A., Ahlquist, N., and Bates, T.: Performance characteristics of a high-sensitivity, three-wavelength, total scatter/backscatter nephelometer, J. Atmos. Ocean. Tech., 13, 967–985, 1996. 1587

Arnott, W., Hamasha, K., Moosmüller, H., Sheridan, P., and Ogren, J.: Towards aerosol light-absorption measurements with a 7-wavelength aethalometer: evaluating with a photoacoustic instrument and 3-wavelength nephelometer, Aerosol Sci. Tech., 39, 17–29, 2005. 1587, 1589, 1592

Backman, J.: Aerosolpartiklars flyktighet och deras optiska egenskaper, Master's thesis, University of Helsinki, Helsinki, 2009. 1586

Birch, M. and Cary, R.: Elemental Carbon-Based Method for Monitoring Occupational Exposures to Particulate Diesel Exhaust, Aerosol Sci. Tech., 25, 221–241, 1996. 1586, 1588

Bond, T. and Bergstrom, R.: Light Absorption by Carbonaceous Particles: An Investigative Review, Aerosol Sci. Tech., 40, 27–67, 2006. 1585, 1596

Bond, T., Anderson, T., and Campbell, D.: Calibration and Intercomparison of Filter-Based Measurements of Visible Light Absorption by Aerosols, Aerosol Sci. Tech., 30, 582–600, 1999. 1585, 1589, 1591, 1596, 1599, 1600

Cabada, J., Khlystov, A., Wittig, A., Pilinis, C., and Pandis, S.: Light Scattering by fine particles during the Pittsburg Air Quality Study: Measurements and modeling, J. Geophys. Res., 109, D16S03, doi:10.1029/2003JD004155, 2004. 1584

Cavalli, F., Viana, M., Yttri, K. E., Genberg, J., and Putaud, J.-P.: Toward a standardised thermal-optical protocol for measuring atmospheric organic and elemental carbon: the EUSAAR protocol, Atmos. Meas. Tech., 3, 79–89, 2010, http://www.atmos-meas-tech.net/3/79/2010/. 1596, 1600

Engler, C., Rose, D., Wehner, B., Wiedensohler, A., Brüggemann, E., Gnauk, T., Spindler, G., Tuch, T., and Birmili, W.: Size distributions of non-volatile particle residuals (D_p¡800 nm) at a rural site in Germany and relation to air mass origin, Atmos. Chem. Phys., 7, 5785–5802, 2007, http://www.atmos-chem-phys.net/7/5785/2007/. 1585, 1596, 1598

Frey, A., Rose, D., Wehner, B., Müller, T., Cheng, Y., A.Wiedensohler, and Virkkula, A.: Application of the Volatility-TDMA Technique to Determine the Number Size Distribution and Mass Concentration of Less Volatile Particles, Aerosol Sci. Tech., 42, 817–828, 2008. 1585, 1597

Hansen, A., Rosen, H., and Novakov, T.: The Aethalometer-An instrument for the real-time measurement of optical absorption by aerosol particles, Sci. Total Environ., 36, 191–196, 1984. 1587

Heintzenberg, J., Wiedensohler, A., Tuch, T., Covert, D., Sheridan, P., Ogren, J., Gras, J., Nessler, R., Kleefeld, C., Kalivitis, N., Aaltonen, V., Wilhelm, R.-T., and Havlicek, M.: Intercomparisons and Aerosol Calibrations of 12 Commercial Integrating Nephelometers of Three Manufacturers, J. Atmos. Ocean. Tech., 23, 902–914, 2005. 1589

Hoppel, W.: Determination of the aerosol size distribution from the mobility distribution of the charged fraction of aerosols, J. Aerosol Sci., 9, 41–54, doi:10.1016/0021-8502(78)90062-9, 1978. 1589

Jacobson, M.: Strong radiative heating due to the mixing state of black carbon in atmospheric aerosols, Nature, 409, 695–697, 2001. 1584, 1585, 1597, 1599

Järvi, L., Hannuniemi, H., Hussein, T., Junninen, H., Aalto, P., Hillamo, R., Mäkelä, T., Keronen, P., Siivola, E., Vesala, T., and Kulmala, M.: The urban measurement station SMEAR III: Continuous monitoring of air pollution and surface-atmosphere interactions in Helsinki, Finland, Boreal Env. Res., 14, 86–109, 2009. 1586

Jokinen, V.: Aerosolihiukkasten ja ilman ionien mittaus differentiaalisella liikkuvuusanalysaattorilla, Report Series in Aerosol Science, 1995. 1587, 1589

Liu, L.-J. S., Slaughter, J., and Larson, T.: Comparison of Light Scattering Devices and Impactors for Particulate Measurements in Indoor, Outdoor, and Personal Environments, Environ. Sci. Technol., 36, 2977–2986, 2002. 1589

Mertes, S., Schröder, F., and Wiedensohler, A.: The particle detection efficiency curve of the TSI-3010 CPC as a function of the temperature difference between saturator and condenser, Aerosol Sci. Tech., 23, 257–261, 1995. 1588, 1589

Mikhailov, E., Vlasenko, S., Podgorny, I., Ramanathan, V., and Corrigan, C.: Optical properties of soot-water drop agglomerates: An experimental study, J. Geophys. Res., 111, 1–16, 2006. 1595, 1609

Miyazaki, Y., Kondo, Y., Sahu, L., Imaru, J., Fukushima, N., and Kanod, M.: Performance of a newly designed continuous soot monitoring system (COSMOS), J. Environ. Monitor., 10, 1195–1201, 2008. 1596

Ogren, J.: Comment on Calibration and Intercomparison of Filter-Based Measurements of Visible Light Absorption by Aerosols, Aerosol Sci. Tech., in print, 2010. 1591, 1596, 1599

Petzold, A. and Schönlinner, M.: Multi-angle absorption photometry – a new method for measurement of aerosol light absorption and atmospheric black carbon, J. Aerosol Sci., 35, 421–441, 2004. 1585, 1596

Philippin, S., Wiedensohler, A., and Stratmann, F.: Measurements of non-volatile fractions of pollution aerosols with an eight-tube volatility tandem differential mobility analyzer (VTDMA-8), J. Aerosol Sci., 35, 185–203, 2004. 1588, 1598

Putaud, J.-P., Raes, F., Dingenen, R., Brüggemann, E., Facchini, M.-C., Decesari, S., Fuzzi, S., Gehrig, R., Hüglin, C., Laj, P., Lorbeer, G., Maenhaut, W., Mihalopoulos, N., Müller, K., Querol, X., Rodriguez, S., Schneider, J., Spindler, G., ten Brink, H., Torseth, K., and Wiedensohler, A.: A European aerosol phenomenology-2:chemical characteristics of particulate matter at kerbside, urban, rural and background sites in Europe, Atmos. Environ., 38, 2579–2595, 2004. 1598

Ramanathan, V. and Carmichael, G.: Global and regional changes due to black carbon, Nat. Geosci., 1, 221–227, doi:10.1038/ngeo156, 2008. 1585

Ramanathan, V., Crutzen, P. J., Kiehl, J. T., and Rosenfeld, D.: Aerosols, Climate, and the Hydrological Cycle, Science, 294, 2119–2124, doi:10.1126/science.1064034, 2001. 1584

Riipinen, I., Pierce, J., Donahue, N., and Pandis, S.: Equilibration time scales of organic aerosol inside thermodenuders: Evaporation kinetics versus thermodynamics, Atmos. Environ., 44, 597–607, 2010. 1585, 1588, 1593, 1596

Rosenfeld, D., Lohmann, U., Raga, G. B., O'Dowd, C. D., Kulmala, M., Fuzzi, S., Reissell, A., and Andreae, M.: Flood or Drought: How Do Aerosols Affect Precipitation?, Science, 321, 1309–1313, doi:10.1126/science.1160606, 2008. 1584

Saathoff, H., Naumanna, K.-H., Schnaitera, M., Schöcka, W., Móhler, O., Schuratha, U., Weingartnerb, E., Gyselb, M., and Baltensperger, U.: Coating of soot and $(NH_4)_2SO_4$ particles by ozonolysis products of α-pinene, J. Aerosol Sci., 34, 1297–1321, 2003. 1585, 1597

Seinfeld, J. and Pandis, S.: Atmospheric Chemistry and Physics – From airpollution to climate change, Wiley-Interscience, 2006. 1591

Snyder, D. and Schauer, J.: An Inter-Comparison of Two Black Carbon Aerosol Instruments and a Semi-Continuous Elemental Carbon Instrument in the Urban Environment, Aerosol Sci. Tech., 41, 463–474, 2007. 1596

Springston, S. and Sedlacek, A.: Noise Characteristics of an Instrumental Particle Absorption Technique, Aerosol Sci. Tech., 41, 1110–1116, 2007. 1594

Stolzenburg, M. and McMurry, P.: An Ultrafine Aerosol Condensation Nucleus Counter, Aerosol Sci. Tech., 14, 48–65, 1991. 1588

Tiitta, P., Miettinen, P., Vaattovaara, P., Joutsensaari, J., Petäjä, T., Virtanen, A., Raatikainen, T., Aalto, P., Portin, H., Romakkaniemi, S., Kokkola, H., Lehtinen, K., Kulmala, M., and Laaksonen, A.: Roadside aerosol study using hygroscopic, organic and volatility TDMAs: Characterization and mixing state, Atmos. Environ., 44, 1–11, 2009. 1585, 1596

Viidanoja, J., Sillanpää, M., Laakia, J., Kerminen, V.-M., Hillamo, R., Aarnio, P., and Koskentalo, T.: Organic and black carbon in PM2.5 and PM10: 1 year of data from an urban site in Helsinki, Finland, Atmos. Environ., 36, 3183–3193, 2002. 1598

Virkkula, A.: Correction of the calibration of the 3-wavelength Particle Soot Absorption Photometer (3λPSAP), Aerosol Sci. Tech., in print, 12, 2010. 1591, 1592, 1598, 1599, 1600, 1605

Virkkula, A., Ahlquist, N., Covert, D., Arnott, W., Sheridan, P., Quinn, P., and Coffman, D.: Modification, Calibration and Field Test of an Instrument for Measuring Light Absorption by Particles, Aerosol Sci. Tech., 39, 68–83, 2005. 1585, 1589, 1590, 1591, 1597, 1599, 1600, 1605

Wehner, B., Philippin, S., and Wiedensohler, A.: Design and calibration of a thermodenuder with an improved heating unit to measure the size-dependent volatile fraction of aerosol particles, J. Aerosol Sci., 33, 1087–1093, 2002. 1585

Wehner, B., Philippin, S., Wiedensohler, A., Scheer, V., and Vogt, R.: Variability of non-volatile fractions of atmospheric aerosol particles with traffic influence, Atmos. Environ., 38, 6081–6090, 2004. 1598

Wehner, B., Petäjä, T., Boy, M., Engler, C., Birmili, W., Tuch, T., Wiedensohler, A., and Kulmala, M.: The contribution of sulfuric acid and non-volatile compounds on the growth of freshly formed atmospheric aerosols, Geophys. Res. Lett., 32, L17810, doi:10.1029/2005GL023827, 2005. 1585

Weingartner, E., Saathoff, H., Schnaiter, M., Streit, N., Bitnar, B., and Baltensperger, U.: Absorption of light by soot particles: determination of the absorption coeffcient by means of aethalometers, J. Aerosol Sci., 34, 1445–1463, 2003. 1589, 1592

Winklmayr, W., Reischl, G., Lindner, A., and Berner, A.: A new electromobility spectrometer for the measurement of aerosol size distributions in the size range of 1 to 1000 nm, J. Aerosol Sci., 22, 289–296, 1991. 1587, 1589

Zhang, R., Khalizov, A. F., Pagels, J., Zhang, D., Xue, H., and McMurry, P.: Variability in morphology, hygroscopicity, and optical properties of soot aerosols during atmospheric processing, P. Natl. A. Sci., 105, 10291–10296, 2008. 1585, 1597

Table 1. Values used in Eq. (6) to calculate the light absorption coefficients with the iterative method described by Virkkula et al. (2005). The coefficients are from Virkkula (2010).

k_0	k_1	h_0	h_1	s
0.358	−0.640	1.17	−0.71	0.017

Table 2. Values used in Eq. (8) to calculate the light absorption coefficients from optical BC measurements with a AE-16 aethalometer. α, M and $\tau_{a,\mathrm{fx}}$ are empirical values.

Wavelength (nm)	SG($\mathrm{m^2\,g^{-1}}$)	100α	M	$\tau_{a,\mathrm{fx}}$
880	16.62	10.38	4.05504	0.15747

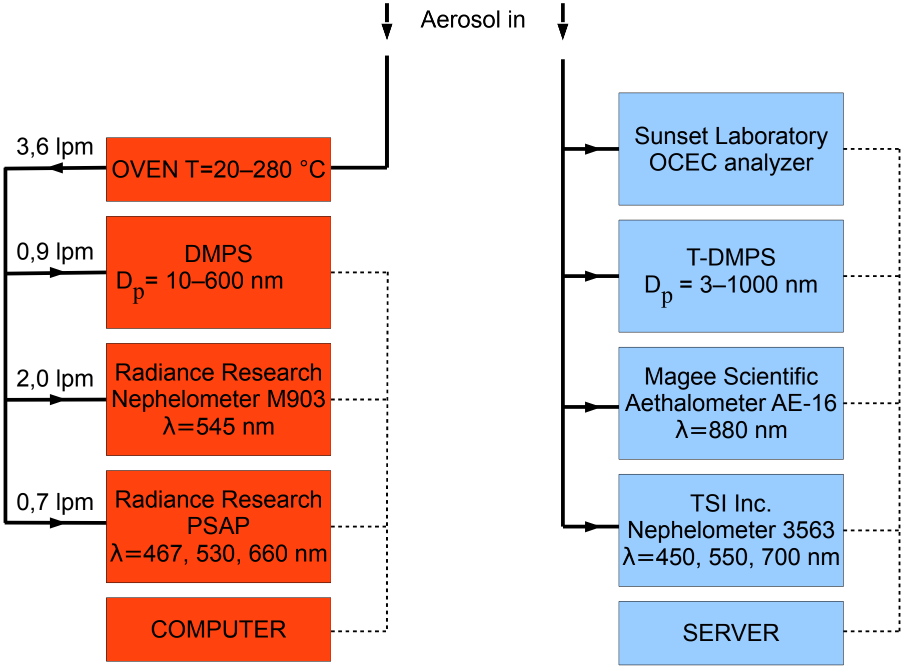

Fig. 1. The system setup used for the experiment at the SMEAR III station to collect the data.

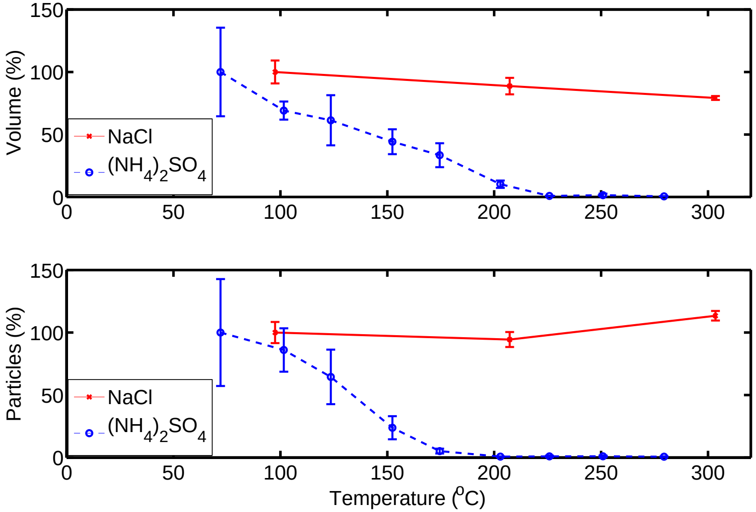

Fig. 2. The volume and particle amount left after the laboratory generated aerosol had been heated to different temperatures in an oven.

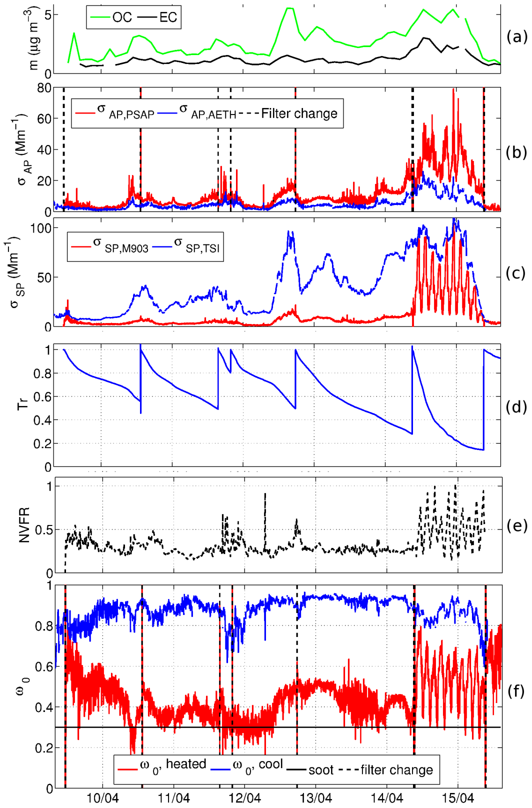

Fig. 3. The values in the picture are **(a)** organic carbon (OC), elemental carbon (EC), **(b)** $\sigma_{AP,PSAP}$ at 545 nm, $\sigma_{AP,AETH}$ at 880 nm **(c)** $\sigma_{SP,M903}$ at 545 nm, $\sigma_{SP,TSI}$ at 550 nm **(d)** PSAP filter transmittance (Tr) at λ= 530 nm **(e)** non-volatile volume fraction remaining (NVFR) and **(f)** single-scattering albedo ω_0 of the cool and the heated urban aerosol were calculated at 880 nm and at 545 nm respectively. The line at ω_0=0.3 is the ω_0 of laboratory generated pure soot (Mikhailov et al., 2006).

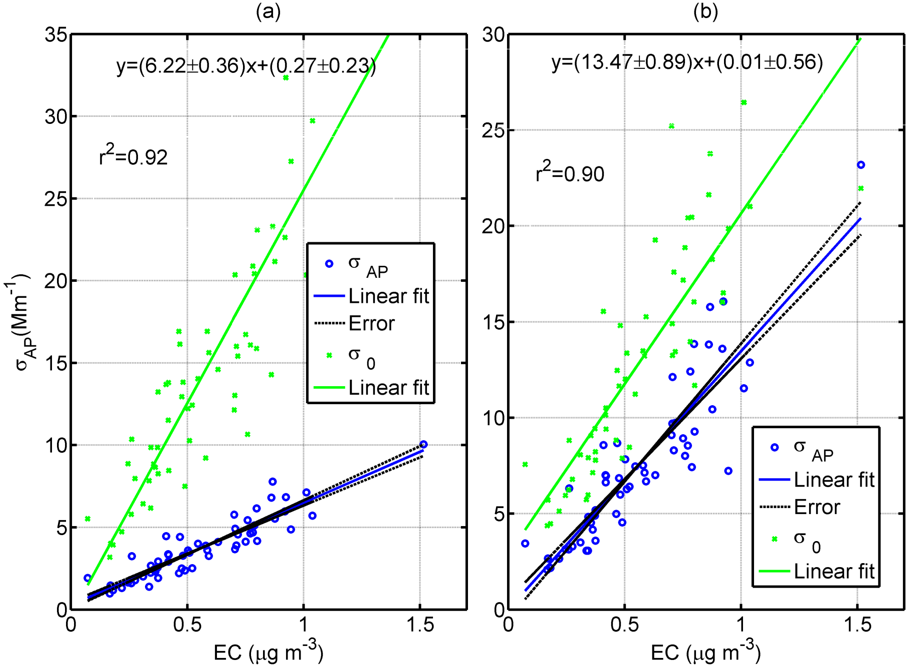

Fig. 4. Mass absorption cross sections (MAC) of soot calculated **(a)** from aethalometer data at a wavelength of 880 mm and OCEC data and **(b)** from PSAP at a wavelength of 545 nm and OCEC data .

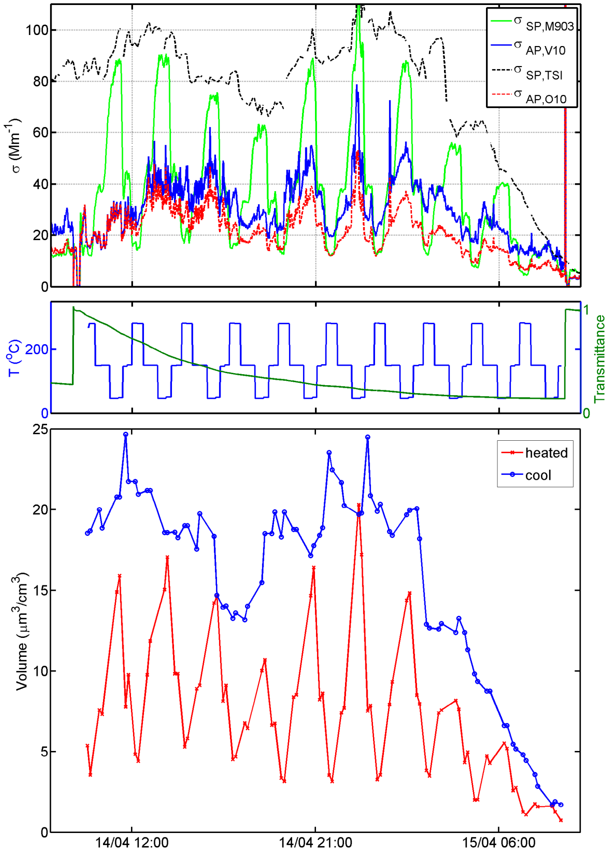

Fig. 5. Light scattering coefficients ($\sigma_{SP,M903}$ at λ=545 nm and $\sigma_{SP,TSI}$ at λ=550 nm), light absorption coefficients ($\sigma_{AP,V10}$ at λ=545 nm and $\sigma_{AP,O10}$ at λ=545 nm), oven temperature, PSAP transmittance at λ=530 nm and the volume of the measured aerosol during the temperature scans.

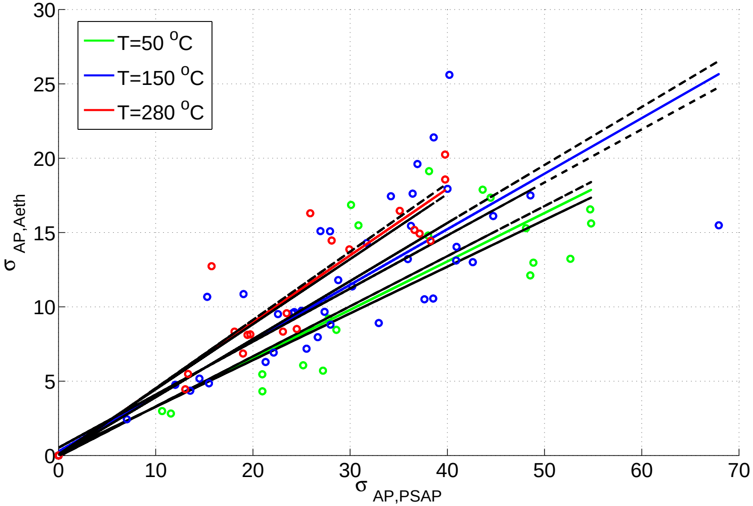

Fig. 6. The temperatures influence on the correlation between the absorption coefficients measurements on the heated aerosol versus the cool aerosol.

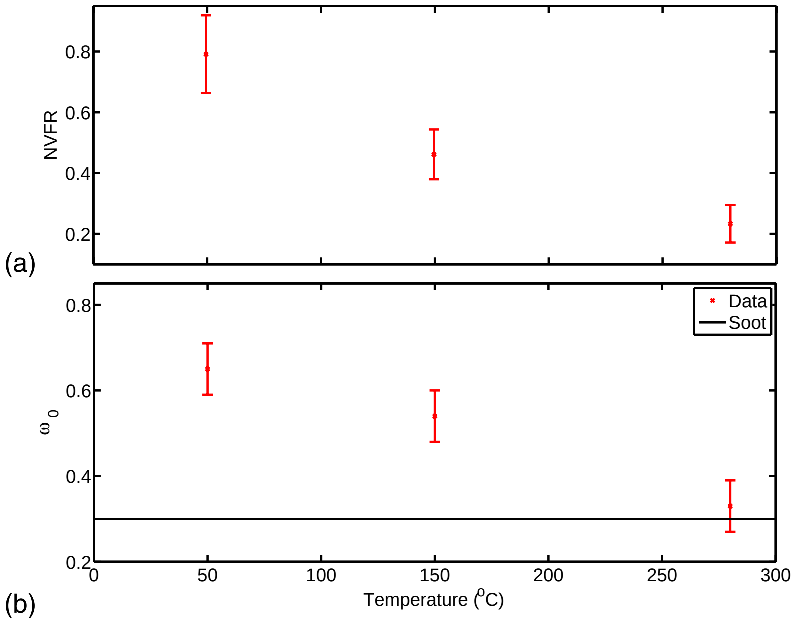

Fig. 7. The amount of **(a)** particle volume left after heating the aerosol to different temperatures and **(b)** the influence of temperature the aerosol was heated to in respect to the darkness of the aerosol as measured between 14 April 2009 LT 10:00 and 15 April 2009 LT 09:00.

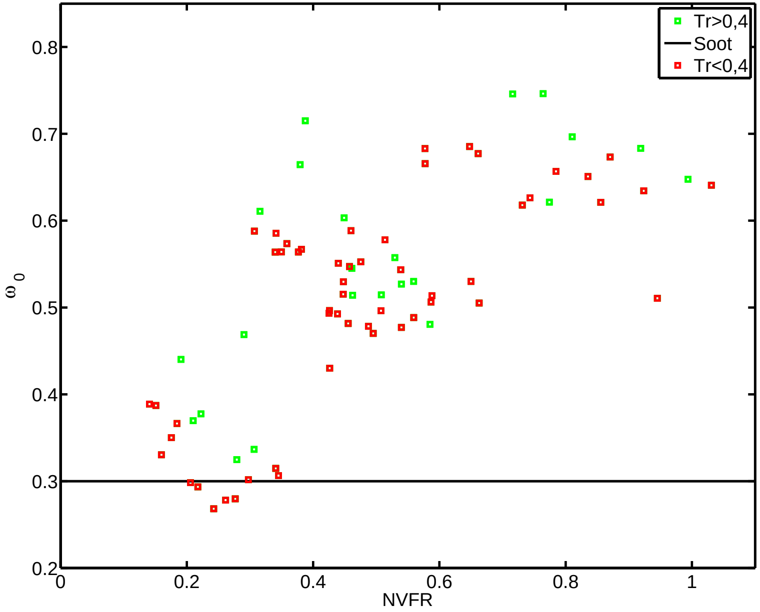

Fig. 8. The influence of volatilisation on the single-scattering albedo (λ=545 nm) of the residual particles of the urban aerosol. The measurements were done on the 14 April LT 10:00 to 15 April LT 09:00.